

A Microfabricated Inductively-Coupled Plasma Generator

J. Hopwood

Department of Electrical and Computer Engineering,
Northeastern University, Boston, MA 02115

ABSTRACT

The design, fabrication, and characterization of a surface micromachined plasma generator is described for the first time. The plasma is sustained without electrodes by inductively coupling a 450 MHz current into a region of low-pressure gas. Both argon and air plasmas have been generated over a range of gas pressures from 0.1 torr to 10 torr (13.3 Pa - 1333 Pa). Typically, the power used to sustain the plasma is 350 mW, although ~1.5 W is required to initiate the discharge. Network analysis of the plasma generator circuit shows that over 99% of the applied RF power can be absorbed by the device. Of this, ~50% is absorbed by the plasma and the remainder of the power is dissipated as ohmic heating. An argon ion current of up to 4.5 mA/cm² has been extracted from the plasma and the electron temperature is 52,000 K at 0.1 torr. This plasma source is intended for electronic excitation of gas samples so that the presence of impurities and toxins may be detected using optical emission spectroscopy.

I. Introduction

A miniaturized device for the production of gas phase electrons, ions, and electronically excited atoms is needed for several MEMS applications including ionizers for micro mass spectrometers, microthrusters¹, plasma displays, and micro atomic emission spectroscopy². The microfabricated plasma generator described in this paper is intended to be used in conjunction with a miniature Fabry-Perot spectrometer³. The complete system of plasma source and spectrometer function as a micro gas analyzer by generating excited atomic and molecular states within a gas sample. The constituents of that sample are then determined based on the wavelength of photons emitted from the plasma following electronic de-excitation.

Perhaps the most commonly used microplasma is found in ac plasma displays. Although the ac plasma display pixel is very compact and relatively simple, the plasma is sustained by high secondary electron yield electrodes. In a chemically-active plasma environment, such as air, the electrodes become contaminated and the pixel fails.⁴ The search for a more robust miniature plasma source has produced the dc microhollow cathode discharge⁵ and a capacitively-coupled microwave plasma⁶. Both of these devices also have electrodes that are exposed to the plasma. The electrodes may become oxidized, chemically etched, or sputter-eroded due to contact with

the plasma. In addition, the electric field that heats the plasma originates and terminates on the electrode surfaces. Charged particles in the plasma are therefore accelerated toward the electrodes, where the particles dissipate a substantial fraction of the supplied power. This mechanism of RF plasma generation is referred to as capacitive coupling. Electrodeless plasma generators, on the other hand, impress an electric field that is tangential to the plasma boundary. This greatly reduces the energetic bombardment of the plasma chamber and improves the efficiency of plasma generation⁷.

The inductively-coupled plasma (ICP) is one type of electrodeless discharge that is now widely used in microfabrication processes due to its relative simplicity, efficient use of power, long lifetime using reactive gases, and low process contamination⁸. The scaling principles needed to reduce the size of a plasma processing ICP (300 mm diam., 13.56 MHz) to that of a MEMS device are described in a previous publication⁹ where it is reported that a 5 mm ICP operates efficiently at ~450 MHz. In reference 9, miniature ICPs were fabricated by etching planar spiral inductors in copper-clad epoxy boards. These prototype generators used discrete capacitors for impedance matching. This paper reports the microfabrication and testing of monolithic, miniaturized ICPs fabricated on glass wafers using surface micromachining¹⁰.

II. Design

The principle of operation for an inductively-coupled plasma is illustrated by the equivalent circuit¹¹ shown in Fig. 1. A planar, spiral inductance (L_C) is driven in series-resonance with a capacitance (C_T) such that a strong RF magnetic field is created near the coil. The plasma forms in a low-pressure chamber positioned adjacent to the spiral coil. An electron current flows through the conductive plasma region so as to oppose the RF magnetic field generated by the coil. The current flow in the plasma is modeled as a single-turn inductor (L_P) and electron collisions are modeled as a resistance (R_{Pi}). Because the coil and the plasma are adjacent, a mutual inductance (M) exists between the coil and the plasma inductance. The equivalent circuit, therefore, looks like a nonideal transformer with a coupling coefficient $k = M/(L_C L_P)^{1/2}$. The RF power source used to drive this miniature plasma has a 50Ω characteristic impedance. C_L is used to cancel the inductive reactance of the circuit and match the impedance of the plasma to the RF source.

A photograph of the plasma generator mounted in a 66-pin hybrid package is shown in Fig. 2 with the three microfabricated circuit elements labeled (L_C , C_T , and C_L). The three-turn coil has a diameter of 5 mm and each turn is 400 μm wide with a 100 μm gap between turns. The inductance is ~ 40 nH and the equivalent series resistance of a 7 μm -thick coil fabricated in gold is $R_C = 0.4 \Omega$ at 450 MHz. The 'tuning'

capacitance (C_T) is chosen to be ~ 3 pF such that the LC-series circuit resonates near 450 MHz. The loop of current within the plasma has a calculated inductance of $L_P \sim 4$ nH. The resistance of the plasma around this inductive loop, which depends on the gas pressure and electron density¹², is the order of $R_{Pi} = 100 \Omega$. Power dissipated in R_{Pi} represents the inductively-coupled power absorbed by the discharge. The transformer coupling coefficient for planar ICP generators¹³ is estimated to be $k=0.2$. Finally, analysis¹⁴ of the equivalent circuit indicates that C_L should be approximately 50 pF.

The microfabricated capacitors that form the impedance matching network for the ICP must be capable of operating at high voltage (100s of volts) and high current (~ 1 A) at a frequency of 450 MHz. The capacitors must also have a good quality factor such that power loss is minimal. Interdigitated capacitors on a glass substrate can meet these criteria and have the added advantage that only a single photomask is needed for fabrication. The width of each digit and the gap between digits was chosen to be 10 μm based on process constraints and electrical breakdown strength¹⁵. The geometry of each capacitor was designed using the method of Alley¹⁶.

The capacitors and inductor are formed from electroplated gold. The thickness of the electroplated film is based on the skin depth of 450 MHz current,

$$d = (2 / m_0 w s)^{1/2} = 3.5 \text{ mm}$$

where m_b and s are the permeability and conductivity of the metal and $w = 2\pi f$. Since the current density decays exponentially from the surface of the metallization, a total plated thickness of two skin depths ($7 \mu\text{m}$) was used. Although copper would decrease the parasitic resistance of the plasma generator, experience shows that copper also oxidizes quickly. These gold structures, however, have operated in unsealed packages for at least 3 months.

III. Fabrication and Packaging

The fabrication sequence, shown in Fig. 3, begins with the sputter deposition of a 30 nm Cr adhesion layer, a 100 nm Au seed layer, and a 30 nm TiW adhesion layer on a $700 \mu\text{m}$ thick glass wafer. A double spin coat of Shipley 4620 photoresist forms a $15 \mu\text{m}$ thick plating mold after exposure and develop. The TiW adhesion layer is etched to expose the Au seed layer from which $7 \mu\text{m}$ -thick gold microstructures are electroplated. The process is completed by stripping the photoresist and etching the initial sputtered layers using the electroplated features as a mask. The fabrication of the plasma source only requires a single photomask, eliminating the need for mask alignment.

The wafers are diced and individual die are bonded into hybrid packages that are cut with rectangular windows as shown in Fig. 2. Two wire bonds connect the rf power input from the package to the die and a third wire bond is used to crossover from the inner turn of

the inductor to C_L . Later versions of the plasma generator will have bonded chambers with microfabricated gas inlets and pumping. So that the plasma behavior can be measured, however, this circuit is bonded to a 9-mm i.d. glass tube as shown in Fig. 4. The glass die forms an endcap for the tube with the circuit components on the outside. The tube connects the plasma generator to a conventional vacuum system that is equipped with a high-accuracy capacitance manometer for pressure measurement. A Langmuir probe may be inserted through the tube and into the plasma to determine its ion density and electron temperature.

IV. Experiment and Results

A. Network Analysis

Ultimately, it is envisioned that the plasma generator will be driven by an integrated circuit oscillator bonded within the hybrid package. For the purpose of experimental characterization, however, precision RF instrumentation is used to supply power to the plasma. Figure 5 shows a block diagram of the RF power supply and measurement system. The power source consists of an HP 8656A (1 MHz-990 MHz) signal generator and an ENI 525LA linear amplifier (gain = 50 dB, 1-500 MHz). The forward power and reflected power are measured using a Narda 3020A dual-directional coupler and HP 435A RF power meter. The ICP is placed in a small, grounded aluminum box. All electrical connections are made with 50Ω coaxial cable.

The network behavior of the microfabricated ICP is plotted in Fig. 6. The one-port S-parameter (S_{11}) is defined as $10\log_{10}(P_r/P_f)$ where P_f is the power of the wave traveling toward the plasma generator and P_r is the power reflected from the plasma. Transmission line losses between the directional coupler and the plasma generator are de-embedded from the measurement. A large negative value of S_{11} indicates that the plasma generator reflects very little power, i.e., the impedance of the plasma generator is matched to the power supply (50 Ω). The upper curve in Fig. 6 shows that S_{11} is poor when no plasma is created in the chamber. A slight dip in S_{11} near 454 MHz indicates the actual resonant frequency of the circuit. The lower curve shows S_{11} when the plasma is ignited. In this particular case the plasma was generated in argon at a pressure of 67 Pa (0.5 Torr, 6.6×10^{-4} atm) and a forward power of $P_f = 350$ mW. The minimum reflected power occurs at 443 MHz where a mere 1.4 mW of power is not absorbed by the plasma generator.

The shift in resonant frequency of the plasma generator observed when the discharge is ignited can be understood by considering the parasitic capacitance between the coil and the plasma. The glass substrate and plasma sheath⁹ act as the dielectric layers of this capacitance. A simple lumped-element model is shown in Fig. 1 where a capacitance (C_{P1}) between the outer turn of the coil and the plasma connects to a second capacitance (C_{P2}) between the plasma and the inner turn. The

intervening resistance (R_{PC}) models the finite conductivity of the plasma as well as power dissipation in the plasma through capacitive coupling. R_{PC} is typically $\sim 10 \Omega$. If a reasonable estimate of 0.15 pF for the equivalent series capacitance of C_{P1} and C_{P2} is used in the model, the S_{11} -minimum frequency is shifted by -11 MHz when the plasma ignites. Results of a SPICE simulation of the equivalent circuit (Fig. 7) verify the change in frequency when the plasma exists near the coil. The operational implications for the observed -11 MHz frequency shift are discussed in the next section.

Ideally, all of the available RF power is coupled to the plasma through inductive heating, and ohmic heating of the electroplated circuit elements is minimal. In addition, since RF power coupled to the plasma through parasitic capacitance primarily enhances ion erosion of the chamber⁷, capacitive heating of the plasma should also be minimized. The equivalent circuit model developed in this work can be used to quantify inductive (R_{Pi}), capacitive (R_{PC}), and ohmic (R_C) power absorption. SPICE analysis of the equivalent circuit model shows (Fig. 7) that most of the power dissipation occurs as inductive heating of the plasma and ohmic heating of the coil, while very little power is capacitively-coupled to the plasma through R_{PC} . Unfortunately, a significant fraction of the RF power absorbed by the plasma generator is dissipated as heat in the coil. Future designs will improve the overall efficiency of plasma generation by reducing R_C .

B. Plasma Ignition

Since the power budget of a MEMS device is limited, the minimum forward power required for plasma initiation was measured as a function of power source frequency and gas pressure in the chamber. Generally, ICPs ignite by capacitively-coupling the high voltage present at the terminals of the unloaded $L_C C_T$ tank circuit into the chamber. It should be noted that once the plasma is established, the inductive power required to sustain the plasma is always considerably lower than the initiation power. Therefore, the RF power supply must be sized to ensure that the discharge starts. In Fig. 8 the plasma is shown to ignite at $P_f = 1.5$ W if the frequency is close to the 'plasma-off' resonance, but the power requirement increases rapidly for higher and lower frequencies. It is interesting to note an advantage of transforming the plasma impedance using an ICP: a 1.5 W RF oscillator ($Z=50\Omega$) only requires a voltage swing of ± 12 v, which is far less than the hundreds of volts needed to initiate other small plasma generators.

The frequency shift caused by the parasitic capacitance between the coil and the plasma may affect the design of the RF supply. A sophisticated RF power source might increase its operating frequency to initiate the plasma and then reduce the frequency to obtain the best power absorption. The more simplistic solution of fixing the frequency to minimize initiation power, however, is also reasonable because S_{11} is still -10 dB at 454

MHz with the plasma on (see Figs. 4 and 6). That is, only 10% of the forward power is reflected from the plasma. The additional electronic complexity needed to gain 10% in plasma source performance may not be warranted for many applications.

This plasma generator is intended to operate at gas pressures well below one atmosphere. Because the gas pumping speed of vacuum MEMS devices will likely be quite limited, we have investigated the performance of the plasma generator as a function of gas pressure. Figure 9 shows the plasma initiation power in argon as a function of gas pressure from 0.1 torr to 10 torr (13 - 1333 Pa). Although it is possible to ignite the discharge over this entire range, it is clearly easier to start the discharge in the vicinity of 1 torr (133 Pa). In a previous publication⁹ it was shown that the plasma ignites most readily when the power source frequency (ω) equals the electron-neutral collision frequency¹⁷ (ν) in the plasma. The electron collision frequency scales linearly with the gas density and therefore with gas pressure. For $\omega = 2\pi \times 450$ MHz, the collision frequency is optimum at an argon pressure of 0.8 torr, which is consistent with the experimental result shown in Fig. 9. If it is desirable to initiate the plasma at a higher pressure, the plasma generator should be designed to operate at a proportionally higher frequency.

The upper curve in Fig. 9 shows that the forward power required to ignite an air plasma is twice that of an Ar plasma. This is

consistent with published data¹⁸ showing that the microwave electric field breakdown strength of argon is 35 V/cm, but the breakdown field increases to 70 V/cm in air. The data of Fig. 9 also show that the optimum pressure for air breakdown is below that of argon. This result is consistent with Ref. 18.

C. *Plasma Properties*

A cylindrical tungsten probe, called a Langmuir probe¹⁹, was inserted into the plasma to measure the electron temperature and the extractable ion current density. An ion current of 1 mA/cm² could be extracted from an argon discharge at $P_f = 350$ mW. The ion current density increased to 4.5 mA/cm² at $P_f = 4$ W. From Langmuir probe theory, this corresponds to an ion density of $\sim 10^{11}$ cm⁻³. The electron temperature was consistent with earlier results⁹, decreasing from 52,000 K (4.5 eV) at 0.1 torr to 25,000 K (2.2 eV) at 1.1 torr. A more complete plasma characterization study can be found elsewhere²⁰.

V. **Conclusion**

For the first time, a surface micromachined inductively-coupled

plasma generator has produced both argon and air discharges. The device is simple to fabricate and robust. The plasma generator has remained functional after three months' exposure to a non-cleanroom environment and operation using inert and oxidizing gases. Presently power is supplied from laboratory instrumentation, but RF power circuits similar to those used in personal wireless communications are more than adequate for initiating and sustaining this plasma. In the future, we will continue to scale the diameter of the coil and plasma chamber toward dimensions of 1 mm or less.

Acknowledgments

The author wishes to thank Mr. Weilin Hu, Mr. Richard Morrison, and Mr. Yu Yin for their assistance, and Mr. Keith Warner and Prof. Nicol McGruer for critical reviews of the manuscript. This work was supported by the National Science Foundation under Grant No. ECS-9701916.

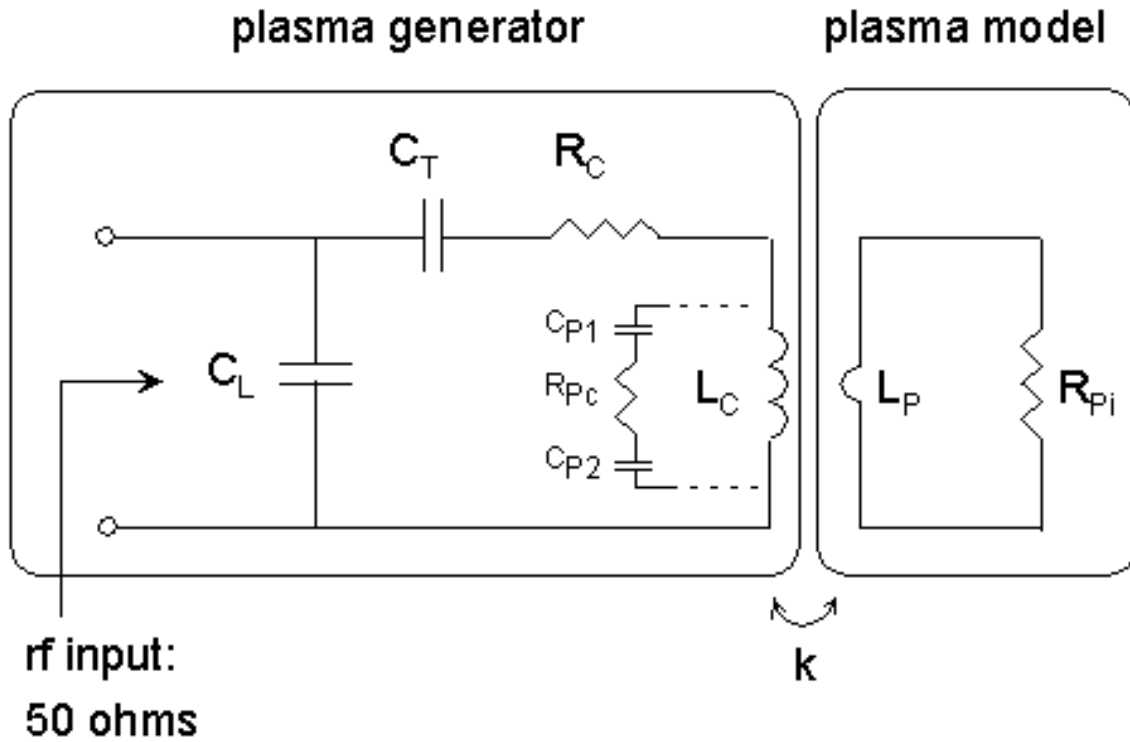


Fig. 1 The equivalent circuit of an inductively-coupled plasma consists of an impedance matching network (C_L and C_T) and an inductive coupler (L_C). The plasma is modeled as a single current loop with inductance L_P and resistance R_{Pi} . The remaining elements are parasitic (see text).

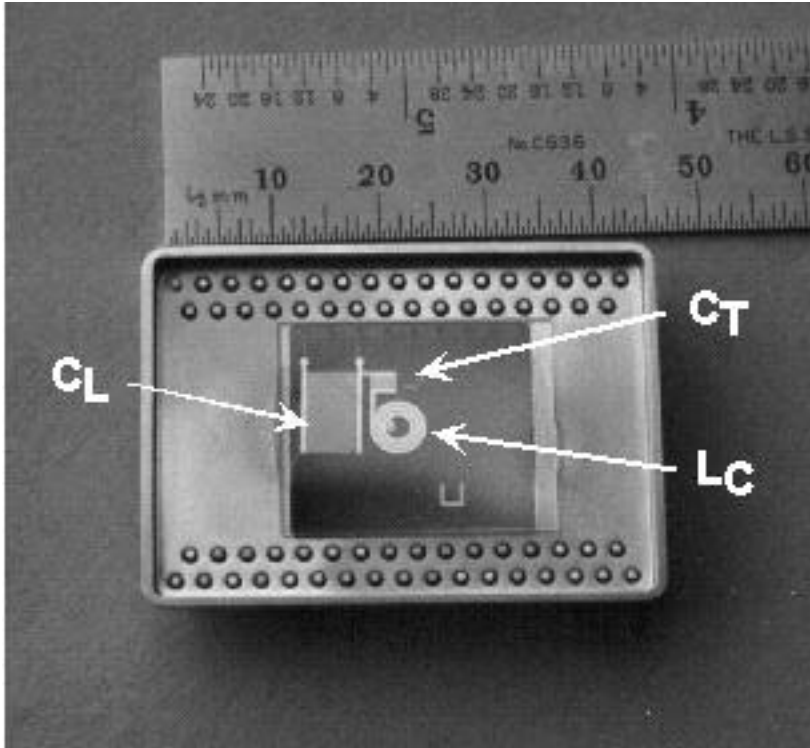


Fig. 2 A plan view shows the microfabricated ICP on a glass die that is bonded in a hybrid package. The impedance matching capacitors and 5 mm diameter inductor are labeled.

Micro-ICP Fabrication Process

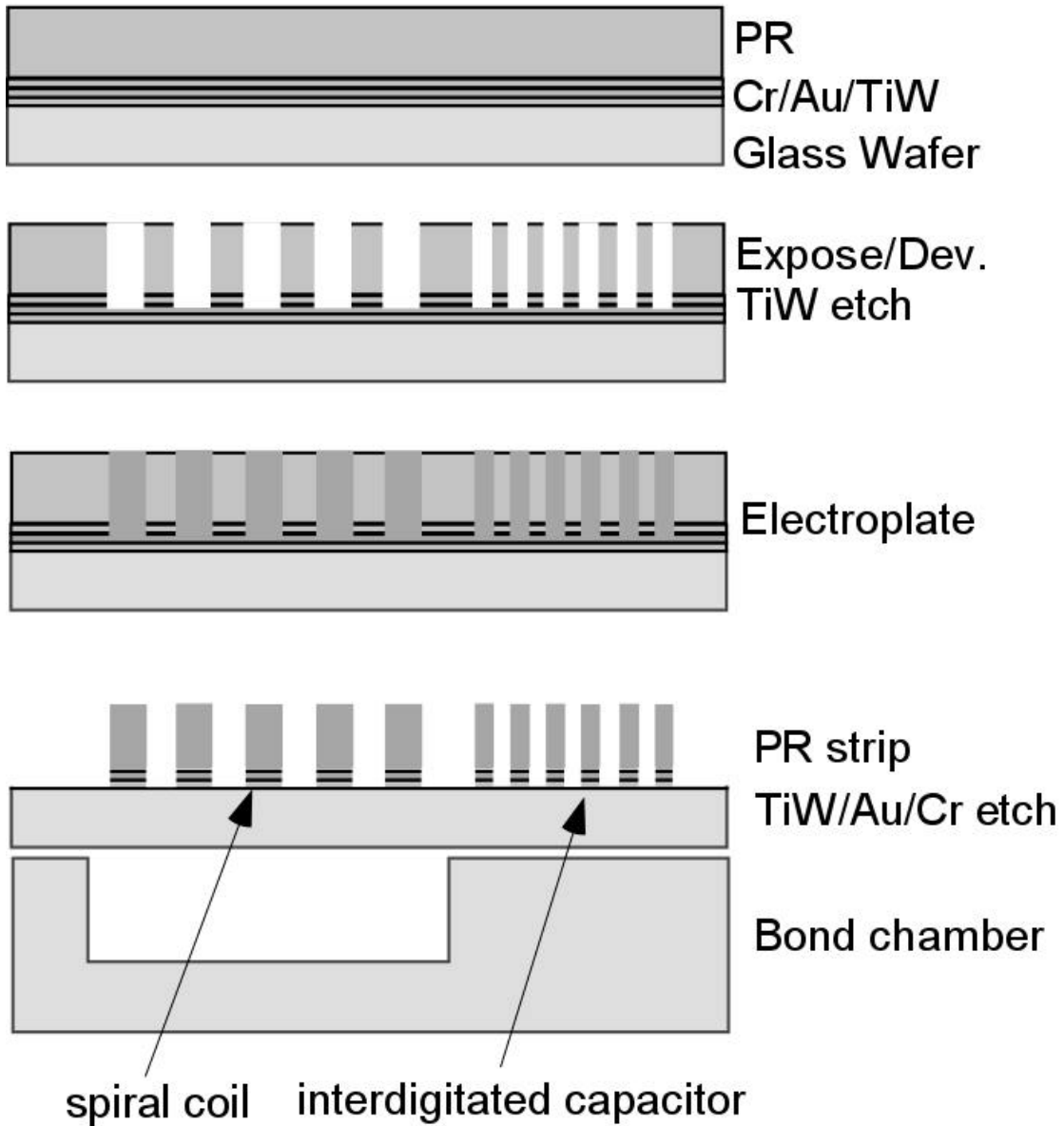


Fig. 3 The single-mask fabrication process for the surface micromachined plasma generator. (In this work a glass tube was used as the plasma chamber.)

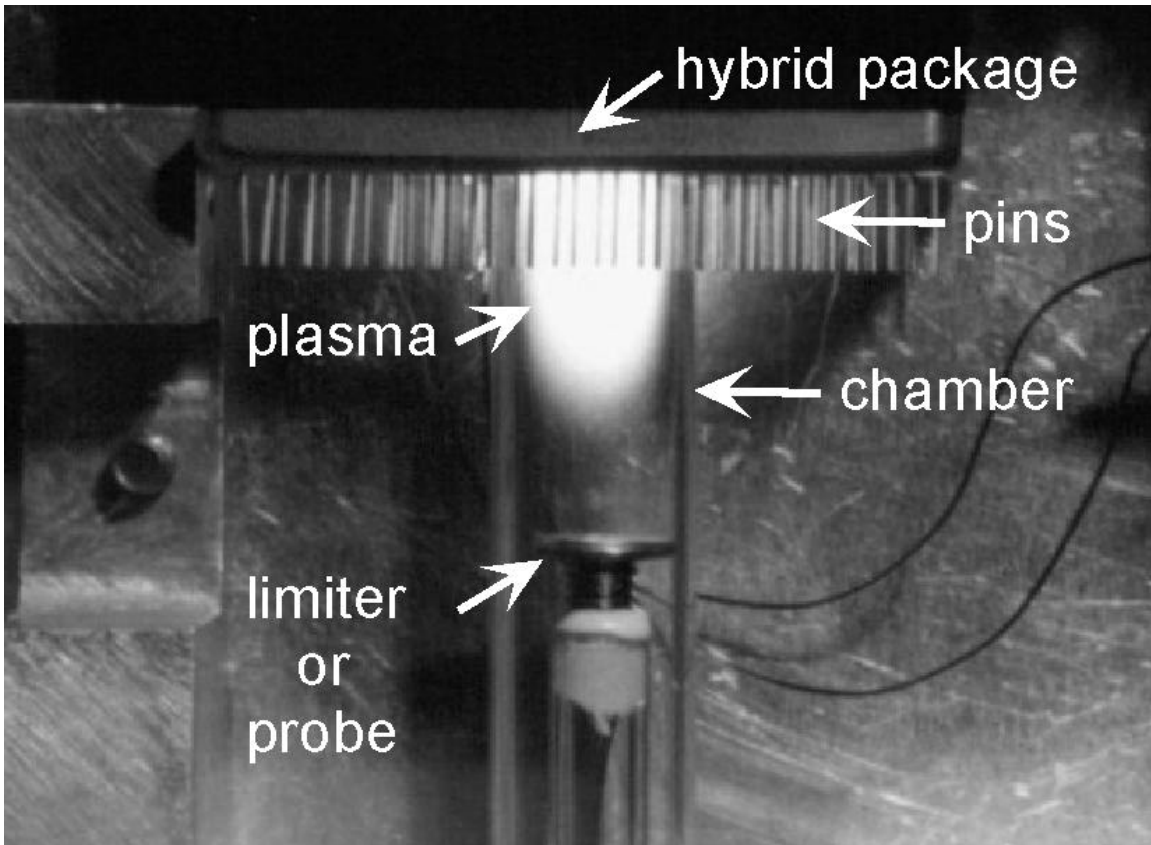


Fig. 4 A side-view of the plasma source shows an argon plasma (8 torr) sustained by 350 mW of rf power at 454 MHz.

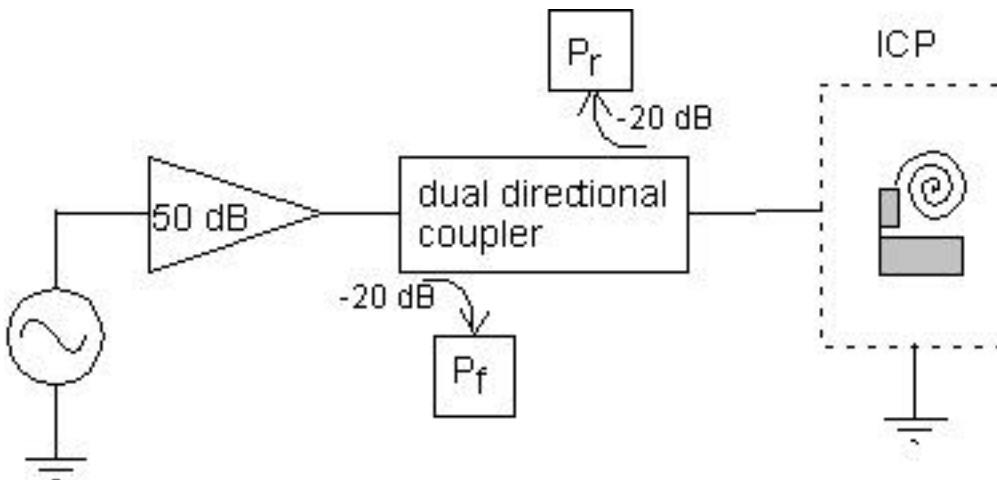


Fig. 5 The test set-up used to supply and measure RF power absorbed and reflected by the plasma.

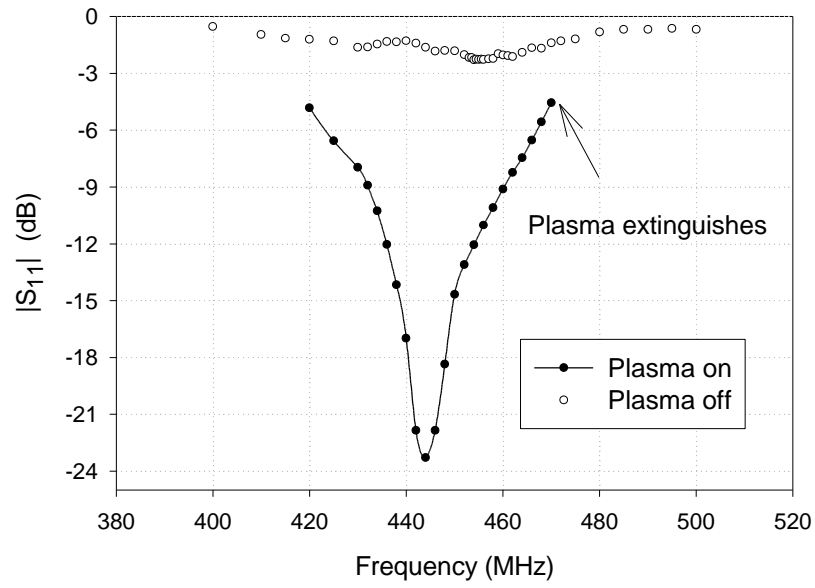
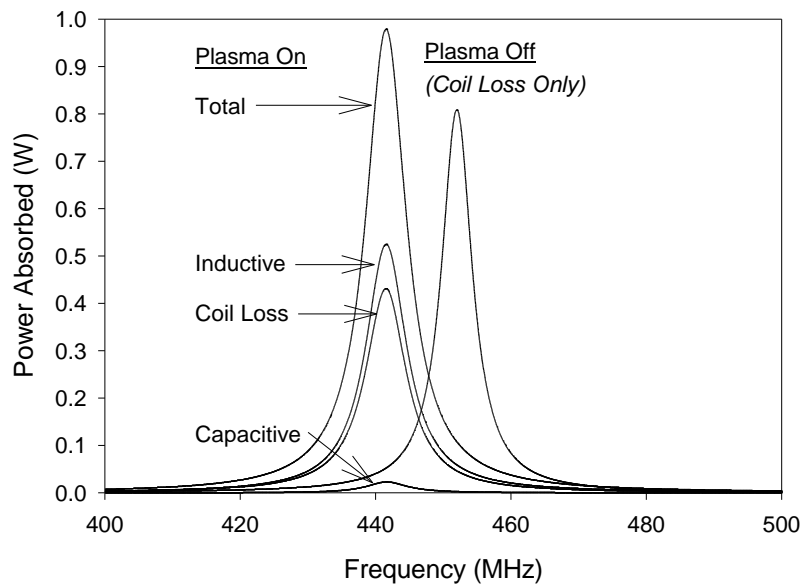


Fig. 6 The one-port S-parameter (S_{11}) as measured with (●) and without (○) a plasma present in the chamber.

Fig. 7 SPICE analysis of the ICP equivalent circuit model shows the shift in resonant frequency caused by capacitive coupling from the coil to the plasma. The distribution of power absorbed by the plasma through inductive and capacitive coupling as well as the power dissipated in the coil (I^2R_C) are also shown for $P_f = 1$ W.



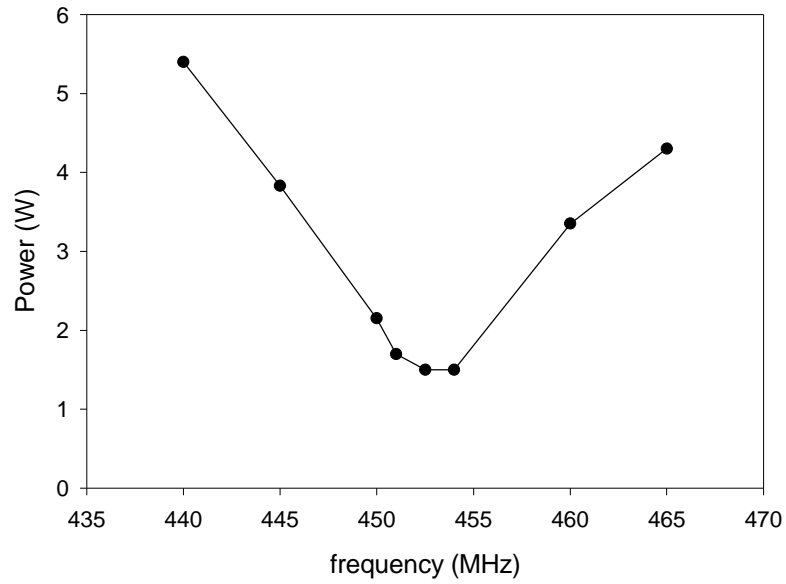
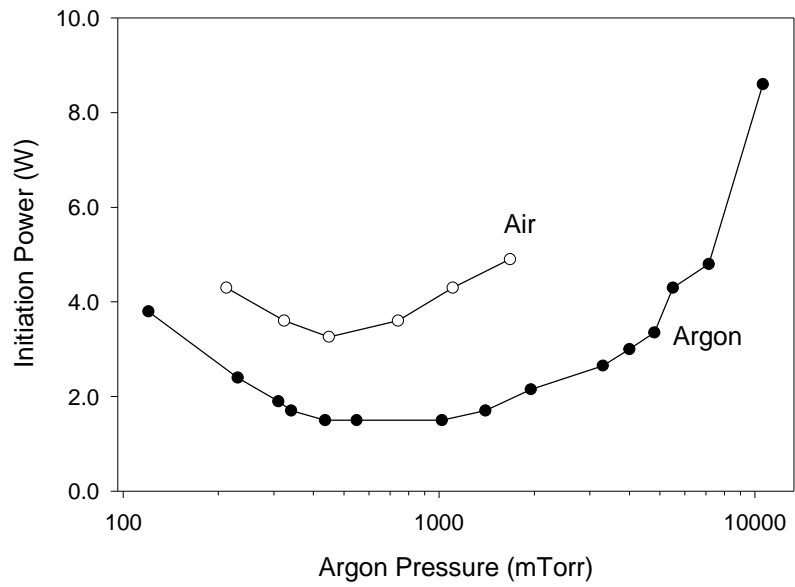


Fig. 8 Plasma initiation occurs at a minimum forward power (P_f) if the frequency is near the 'plasma-off' resonance of the circuit (454 MHz).

Fig. 9 The forward power (P_f) necessary to initiate the discharge is minimum between 0.5 and 1 torr. Once the plasma is lit, only a few hundred milliwatts are needed to sustain the discharge.



REFERENCES

- ¹ J. Mueller, J. R. Brophy, J. E. Polk, and J. J. Blandino, "The JPL ion thruster-on-a-chip concept," 7th NASA-OSAT Advanced Space Propulsion Workshop, Pasadena, CA, April 10, 1996.
- ² B. S. Ross, D. M. Chambers, G. H. Vickers, P. Yang and G. M. Hieftje, "Characterisation of a 9-mm torch for inductively coupled plasma mass spectrometry," *J. Anal. At. Spectrom.*, vol. 5, pp. 351-358, 1990.
- ³ P.M. Zavracky, K. L. Denis, H.K. Xie, R. Grace, T. Wester, "A Micromachined Scanning Fabry-Perot Interferometer," *Proceedings of SPIE*, vol. 3514, pp. xxx-yyy, Nov. 1998.
- ⁴ R.M. Caloi and C. Carretti, "Getters and gettering in plasma display panels," *J. Vac. Sci. Technol. A*, vol. 16, pp. 1991-1996, 1998.
- ⁵ K. H. Schoenbach, C. A. Verhappen, T. Tessnow, F. E. Peterskin, and W. W. Byszewski, "Microhollow cathode discharges," *Appl. Phys. Lett.*, vol. 68, no. 1, pp. 13-15, 1996.
- ⁶ P. Siebert, G. Petzold, A. Hellenbart, J. Muller, "Surface microstructure/miniature mass spectrometer: processing and applications," *Appl. Phys. A*, vol. 67, pp. 155-160, 1998.
- ⁷ M. A. Lieberman and A. J. Lichtenberg, *Principals of Plasma Discharges and Materials Processing*, New York: Wiley, 1994, p. 308-309.
- ⁸ J. Hopwood, "Review of inductively coupled plasmas for plasma processing," *Plasma Sources Science and Technology*, vol. 1, no. 2, pp. 109-116, 1992.
- ⁹ Y. Yin, J. Messier, and J. Hopwood, "Miniaturization of inductively coupled plasma sources," *IEEE Trans. Plasma Sci.*, vol. 27, no. 5, pp. 1516-1524, 1999.
- ¹⁰ "Monolithic miniaturized inductively coupled plasma source," J. Hopwood, U.S. Patent No. 5,942,855 (August 24, 1999).
- ¹¹ R. B. Piejak, V. A. Godyak, and B. M. Alexandrovich, "A simple analysis of an inductive RF discharge," *Plasma Sources Sci. Technol.*, vol. 1, pp. 179-186 1992.
- ¹² M. A. Lieberman and A. J. Lichtenberg, *Principals of Plasma Discharges and Materials Processing*, New York: Wiley, 1994, p. 392.
- ¹³ L. J. Mahoney, Ph. D. Thesis, University of Wisconsin-Madison, p.51 (1994).

- ¹⁴ M. A. Lieberman and A. J. Lichtenberg, *Principals of Plasma Discharges and Materials Processing*, New York: Wiley, 1994, p. 396.
- ¹⁵ J. D. Craggs, "High-frequency Breakdown of Gases," in *Electrical Breakdown of Gases*, Meeks and Grayh, Eds., New York: Wiley, 1973, pp.689-705.
- ¹⁶ G. D. Alley, "Interdigital capacitors and their application to lumped-element microwave integrated circuits," *IEEE Trans. on Microwave Theory and Tech.*, vol. MTT-18, no. 12, pp. 1028-1033, 1970.
- ¹⁷ M. A. Lieberman and A. J. Lichtenberg, *Principals of Plasma Discharges and Materials Processing*, New York: Wiley, 1994, p. 80.
- ¹⁸ S. C. Brown, *Basic Data of Plasma Physics*, Cambridge, MA: The MIT Press, 1966, p. 252.
- ¹⁹ I.D. Sudit and R.C. Woods, *J. Appl. Phys.* vol. **76**, pp. 4488, 1994.
- ²⁰ J. Hopwood, *J. Vac. Sci. Technol.*, in preparation.